防蝕工程 第八卷第三期 第130～139頁 民國83年9月
Journal of Chinese Corrosion Engineering, Vol.8, No.3, PP.130～139(1994)

英高鎳600合金在外加陰極電位的氯化鈉溶液中的疲勞裂縫生長行爲

賀瑞庭 喻冀平

Fatigue Crack Growth Behavior of Alloy 60 in NaCl Solution at Cathodic Potential

Jui-Ting Ho and Ge-Ping Yu

摘 要

工廠退火的600合金在室溫25°C，0.1M氯化鈉溶液中的疲勞裂縫生長速率受外加電位、負荷頻率及負荷比的引影響，在外加陰極電位(-1300mV$_{SCE}$)下，疲勞裂縫生長速率隨負荷頻率的降低及負荷比的提高而增加，在低於0.1Hz的負荷頻率有裂縫生長加速的現象，且此現象隨負荷比的提高而變得更加顯著。負荷比的效應採用Walker的模式來說明，並推導出一保守的上限邊界。斷裂面顯示有二次裂縫存在及穿晶破裂模式，對於可能的氫促進破裂的機制有所探討。

關鍵詞：疲勞裂縫生長、600合金、氯化鈉、陰極電位、氫促進破裂

ABSTRACT

The fatigue crack growth (FCG) rates of mill annealed Alloy 60 in 0.1M NaCl soluton, 25°C, were studied by a fracture mechanics test method. They were affected by the applied potential, load frequency and load ratio. At an applied cathodic potential of -1300mV$_{SCE}$, the FCG rates increased with lowering the load frequency and with increasing the load ratio. The enhanced FCG rate was found in the lower load frequencies (≤ 0.1Hz) and was more significant with increasing the load ratio. The load ratio effects were successfully accounted for employment of the Walker model. The secondary cracks and transgranular fracture modes were observed on the fractured surfaces with applied cathodic potential. The possible hydrogen-assisted cracking mechanism on enhancing the FCG rates of Alloy 600 cathodically charged in 0.1M NaCl solution, 25°C, was discussed in this paper.

Keywords: Fatigue Crack Growth, Alloy 600, Sodium Chloride, Cathodic Potential, Hydrogen- Assisted Cracking.

INTRODUCTION

Alloy 600 is an austenitic Ni-base alloy which finds extensive industrial applications as a heat exchanger tube material because of its excellent corrosion resistance, adequate thermal conductivity, and good mechanical properties. The fatigue cracking problems occurred in steam generator (S.G.) tubes of pressurized water reactors (PWR) have been observed for several years. The most likely regions for vibration and possible fatigue failure of the S.G. tubes occurred just above the tube sheet and also in the U-bend region where the flow velocities of the primary coolant were

國立清華大學核子工程與工程物理研究所
Department of Nuclear Engineering and Engineering Physics, National Tsing hua University, hsinchu 300, Taiwan, R.O.C.

the highest and the cross flow from the secondary coolant side was significant[1]. NaCl is easy to be found in the nuclear power plant cooling with sea water, and exists in the secondary coolant because the possible leakage of sea water from the condenser. The Alloy 600 tubes in present-day steam generators pass through carbon steel support plates, a galvanic cell may be established upon contact.

The Alloy 600 tube is cathodic relative to the carbon steel support plate. At room temperature, the reduction of protons to form atomic hydrogen on the tube surface is the likely cathodic reaction. Adsorbed atomic hydrogen can either recombine to form molecular hydrogen, or become absorbed into the metal. The uncombined or atomic hydrogen is the possible source of embrittlement.

Fatigue crack growth testing of Alloy 600 in aqueous solutions at cathodic potentials have previously received little investigation, especially in the NaCl solution. Was et al.[2] performed FCG tests in 1N H_2SO_4 solution under the applied cathodic potential, -700mV$_{SCE}$, and indicated that both lowering the load frequency (10Hz→1Hz) and raising the load ratio (0.05→0.60) would result in a larger FCG rate. Shalaby et al.[3] found the fatigue life of solution annealed Alloy 600 in 4M NaCl solution at room temperature decreased by increasing the applied potential from -900mV$_{SCE}$ (cathodic range) to -400mV$_{SCE}$ (passive range) and to -100mV$_{SCE}$ (above the pitting potential). In addition to the fatigue testing, it also has been found that the presence of dissolved hydrogen in pure water increases the susceptibility to intergranular stress corrosion cracking (IGSCC) of Alloy 600 and accelerates the crack growth rate[4, 5].

The S.G. tubes experience fatigue from pressure fluctuations, secondary water flow, thermal cycling and the startup-shutdown process. This leads to load cycles that may vary in frequency from 10^2 Hz (flow vibrations) to 10^{-7} Hz (shutdown-startup associated loads)[2]. Fatigue crack growth tests are selected based on the rationale that with 60 miles of tubing per S.G., flaws are likely to be present at the start-up, and therefore, it is the propagation stage rather than the initiation stage that is most relevant to the problem.

The purpose of this study lies in investigating the fatigue crack growth behavior of mill annealed Alloy 600 in 0.1M NaCl solution at cathodic potential (-1300mV$_{SCE}$) as a function of load frequency and load ratio, and to find the possible hydrogen-assisted cracking mechanism during fatigue testing. The FCG rate tests at room temperature are for the basic research of fatigue behavior of Alloy 600 in aqueous solution, in spite of the actual structure in PWR power plant are subjected to high temperature.

EXPERIMENTAL PROCEDURES

The chemical composition and the mechanical properties of the mill annealed Alloy 600 used are provided in Table 1 and Table 2, respectively. FCG rate tests were conducted on 12.7 mm thick compact tension (CT) specimens. Details of the specimen geometrical configuration are illustrated in Figure 1 and are in accordance with ASTM specification E-647-83[6]. Prior to fatigue tests, all of the specimens were polished with 600 grit silicon carbide paper, rinsed with water in ultrasonic oscillator, air dried and cleaned with acetone. Fatigue precracking was made to extend the 12.7 mm (0.5 inch) machined notch a further 3 mm in air. The tests were conducted with a sinusoidal loading waveform in the load control made and a load ratio ($R=P_{min}/P_{max}$) of 0.1, using a 100 kN capacity closed-loop servohydraulic machine. P_{max} was maintained at a constant value of 16 kN during each FCG rate test.

FCG rate tests in solution were conducted in a transparent acrylic cell containing 1500 ml solution at 25°C, as shown in Figure 2. A water pump was immersed in the water tank for recirculating the test solution through the pipe with a 10 l/min flow velocity. High-purity analytical-grade NaCl and deionized water (>15MΩ•cm) were employed for preparing the testing solutions, and the test solutions were air saturated. When applied potential tests were performed, the CT specimens were coated with a layer of silicone rubber, with only an area of 30 by 5 mm^2 ahead of the machined notch on both sides of the specimen being exposed to the solution. The potential of the specimen, -1300mV$_{SCE}$, was applied with respect to

Table 1. The chemical composition of mill annealed Alloy 600

Ni	Cr	Fe	C	Cu	Si	Mn	S
74.25	16.24	8.71	0.07	0.25	0.24	0.24	0.001

Table 2. Mechanical properties of mill annealed Alloy 600

0.2% Yield Strength (Mpa)	Ultimate Tensile Strength (MPa)	Elong. (%)	Rct. RA (%)	Vickers Hardness (HV)	Grain Size (μm)
235.7	628.2	63	43	161.7	68

an external saturated calomel electrode (SCE). A pair of platinum wires were used as the counter electrodes, which were located on both sides of the test specimen.

Fatigue crack lengths on both sides of the polished specimen surfaces were measured to an accuracy of 0.01 mm by using a traveling microscope. The crack length of the specimen was:

$$a = a_0 + \frac{d_1 + d_2}{2} \quad (1)$$

a_0: initial crack length (=12.7 mm)

d_1, d_2: crack length on each side of the specimen

All of the FCG rate curves were constructed by the seven point incremental polynomial method to convert crack length, a, as a function of number of cycles, N, to fatigue crack growth rate, da/dN, vs. stress intensity range, ΔK. ΔK of the CT specimens was calculated as follows(6):

$$\Delta K = \frac{\Delta P}{B\sqrt{W}} \frac{(2+\alpha)}{(1+\alpha)^{3/2}} (0.886+4.64\alpha-13.32\alpha^2+14.72\alpha^3-5.6\alpha^4) \quad (2)$$

where ΔP: the applied load range ($=P_{max}-P_{min}$)

B: specimen thickness

W: specimen width

α: a/W

Following fatigue testing, the fractured surfaces of the CT specimen were examined via a scanning

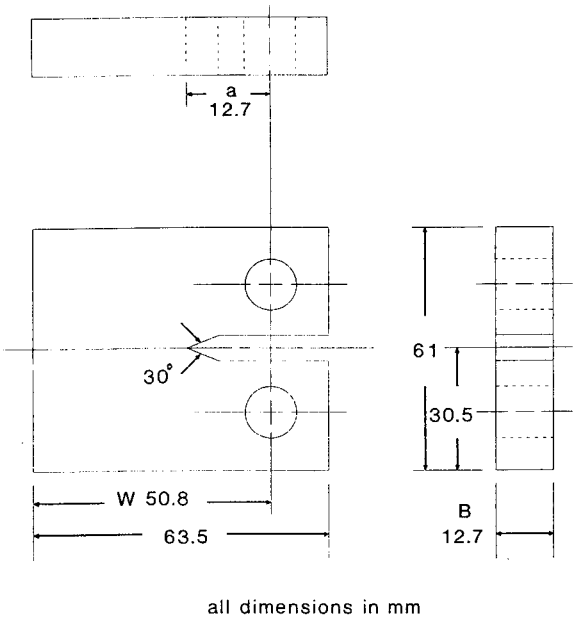

Figure 1. The dimensions of compact tension specimen.

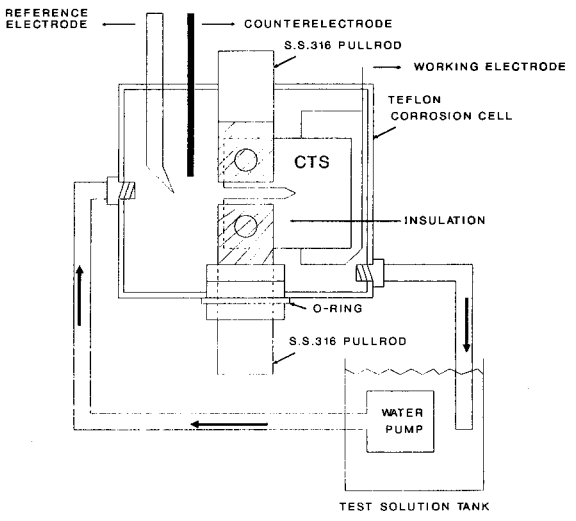

Figure 2. Schematic diagram of fatigue crack growth rate test.

electron microscope (SEM).

In addition to the fatigue tests, tension tests were performed on the rectangular specimen, with a gauge length of 25mm, in 0.1M NaCl solution at 25°C, -1300mV$_{SCE}$, and strain rates of 10^{-3} and 10^{-4} s^{-1}.

RESULTS

The FCG rates of Alloy 600, R=0.1, in 0.1M NaCl solution, 25°C, at -1300mV$_{SCE}$ are shown in Figure 3. At -1300mV$_{SCE}$ (cathodic potential), large amounts of hydrogen are liberated from the specimen. The hydrogen bubbles tend to nucleate preferentially on the crack surfaces as opposed to the polished specimen outer surface. Compared with the air environment, the FCG rates (R=0.1, f=1Hz) in NaCl solution at open circuit potential (O.C.P., -123mV$_{SCE}$) and -1300 mV$_{SCE}$ are about 1.5 to 2 times larger than the FCG rate inair in the lower ΔK range (<23 MPa $\sqrt{m}$). At ΔK=22 MPa $\sqrt{m}$, the crack growth rate was 1.4×10^{-7}m/cycle in air and was 2.7×10^{-7}m/cycle in 0.1M NaCl solution with and without applied cathodic potential. As the ΔK increases, the FCG rates, f=1Hz, in solution environments are almost similar to the rate in air. In 0.1M NaCl solution, 25°C, the FCG rates, R=0.1, f=1Hz, at O.C.P. and -1300mV$_{SCE}$ are almost the same in the whole ΔK range. Figure 3 also shows that the FCG rates (R=0.1, V=-1300mV$_{SCE}$) increase with decrease in frequency from 1Hz to 0.03Hz, although the trend is not significant.

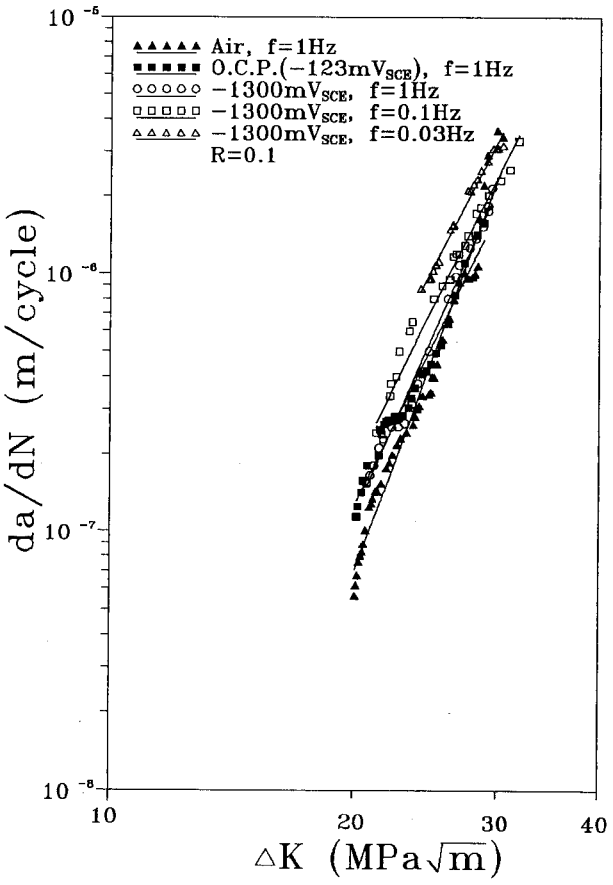

Figure 3. The FCG rates of Alloy 600, R=0.1, in air and 0.1 NaCl solution at open circuit potential, O.C.P.=-123mV$_{SCE}$, f=1Hz, and cathodic potential, -1300mV$_{SCE}$, f=0.03-1Hz, 25°C.

The dependence of da/dN on frequency at ΔK=24.2 MPa$\sqrt{m}$ and ΔK=28.2 MPa$\sqrt{m}$ in NaCl solution at -1300mV$_{SCE}$ is shown in Figure 4(a). It depicts that the values of da/dN increase with decrease in frequency at the above two equivalent stress intensity factor ranges. The relationship of crack growth rate with frequency can also be analyzed in terms of the dependence of da/dt (time based crack growth rate) on f (frequency). The relationship between da/dt and frequency for ΔK=24.2 MPa$\sqrt{m}$ and ΔK=28.2 MPa$\sqrt{m}$ are shown in Figure 4(b). These data show that the crack growth rates in 0.1M NaCl solution, 25°C, at -1300mV$_{SCE}$ become increasingly greater than the corresponding cycle dependent FCG rates (the slope of the log (da/dt) vs. log (f) curve equals to 1, represented by the dashed lines) as the frequency decreases.

The FCG rates of Alloy 600 with different load ratio in air, f=1Hz, and in 0.1M NaCl solution, 25°C, with an applied potential of -1300mV$_{SCE}$, f=0.03-1Hz, are depicted in Figure 5. This figure indicates that the FCG rates increase as R was raised from 0.2 to 0.5 when extrapolating the curve of R=0.5 to the higher ΔK region in air and 0.1M NaCl solution. At the same load ratio, the FCG rates, f=0.1Hz, in 0.1M NaCl solution at -1300 mV$_{SCE}$ were significantly larger than the FCG rates, f=1Hz, in air and 0.1M NaCl solution at -1300mV$_{SCE}$, especially in R≥0.2. At R=0.5 condition, the enhancement of the FCG rates in 0.1M NaCl solution, 25°C, at -1300mV$_{SCE}$ not only existed in the f=0.1Hz condition, but also was found in f=1Hz condition.

Following fatigue testing, the fracture surface was cleaned and examined by SEM. Figure 6 de-

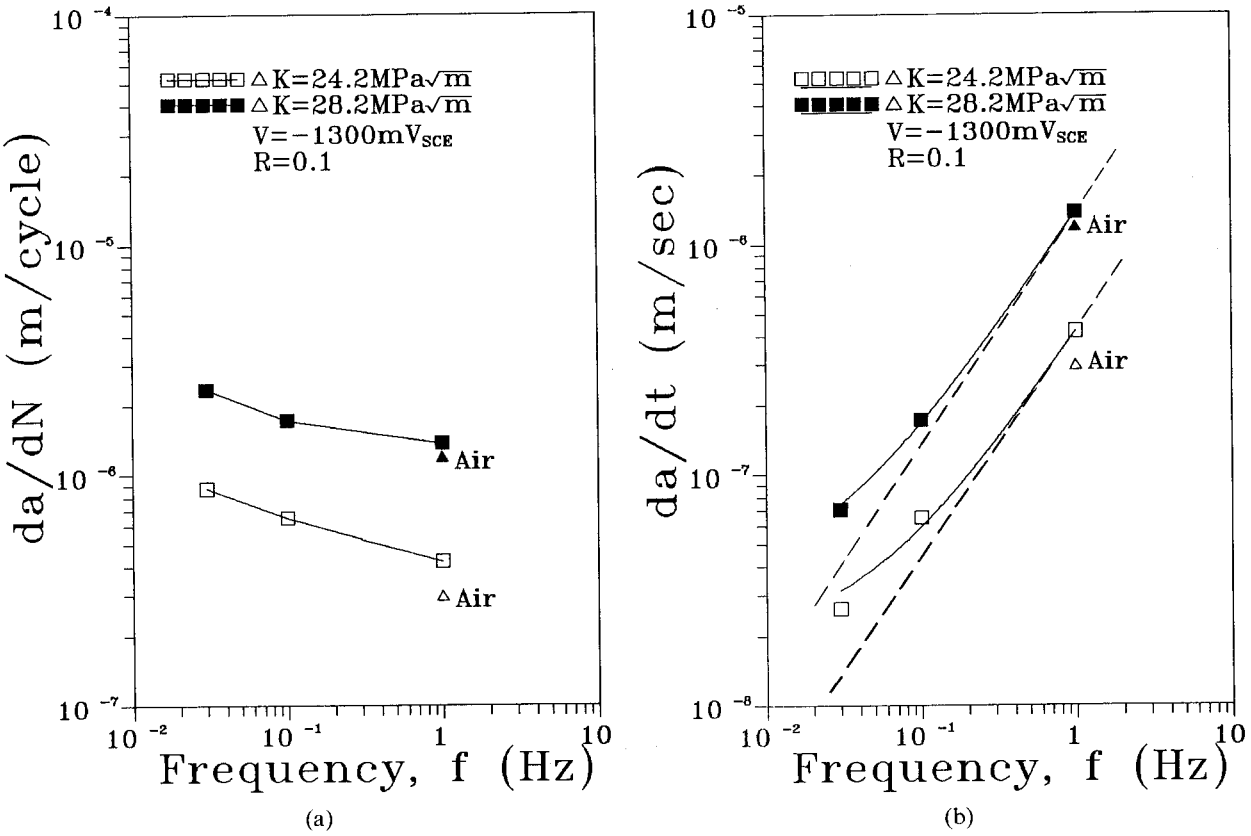

Figure 4. Effect of load frequency on (a) the FCG rates, da/dN, and (b) the time based FCG rates, da/dt, of Alloy 600, R=0.1, in 0.1M NaCl solution, 25°C, with an applied potential of -1300mV$_{SCE}$, at ΔK=24.2 MPa$\sqrt{m}$ and ΔK=28.2 MPa$\sqrt{m}$.

picts the typical fractographic features, and the failure mode is transgranular. The corrosion products were found on the fracture surface tested in NaCl solution, O.C.P., at low ΔK values but not found in air. Fatigue striations were easily observed at the high values of ΔK (toward end of test), Figures 6(a) and 6(b), but were often indistinct at low ΔK values (near start of test). In 0.1M NaCl solution at -1300mV$_{SCE}$, f=1Hz, the secondary cracks and fatigue striations were found on the fracture surface [Figures 6(c) and 6(d)]; but in f=0.1Hz condition, fatigue striations were indistinguishable and many secondary cracks were still observed on the fracture [Figures 6(e) and 6(f)]. The appearance of the secondary crack is the characterization of brittle fracture, and it should result from the effect of hydrogen during the fracture process. As expected, dimple fracture [Figure 6(g)] was observed during final overload failure.

In the tension test, strain rates of 10^{-3} and 10^{-4} s^{-1}, the mechanical properties (yield strength, ultimate tensile strength,...etc.) in 0.1M NaCl solution at 25°C and -1300mV$_{SCE}$, shown in Table 3, were almost the same as the data in air, dipicted in Table 2, and dimple rupture (the same observation in air) was found on the fracture surface. The tension test was also conducted on the precracked CT specimen in the same environment, at a crosshead speed of 2.5×10^{-2} mm/sec, and the fractographs still revealed the ductile fracture.

DISCUSSION

The previous study indicated that the environmental enhancement on the FCG rates of Alloy 600 in NaCl solution at room temperature were not found at different solution concentration, load frequency and load ratio[7]. In this study, the test results show that the acceleration of the FCG rates as the load frequency decreases when specimens are cathodically charged at -1300mV$_{SCE}$ dur-

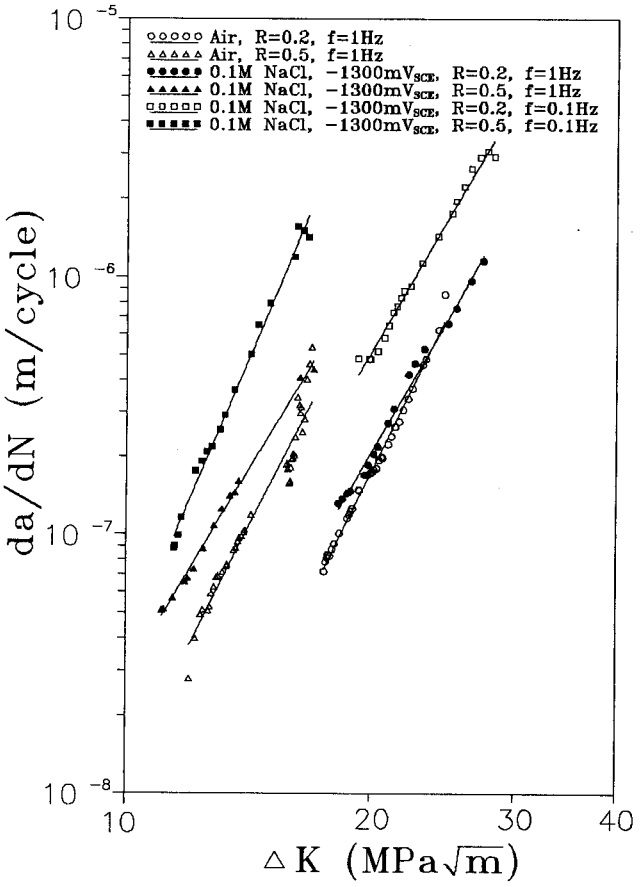

Figure 5. The FCG rates of Alloy 600 at R=0.2 and 0.5 in air, f=1Hz, and in 0.1M NaCl soution, 25°C, at -1300mV$_{SCE}$, f=0.1 and 1Hz.

ing testing. It is postulated that at cathodic potentials, hydrogen-assisted cracking is the possible cause of FCG rate enhancement.

The enhancement of FCG rates with decreasing load frequency at cathodic charging strongly suggests a time dependent hydrogen supply effect, i.e., the longer testing time in the low frequency condition makes a larger amount hydrogen retained in the crack. Results show that at a cathodic potential of -1300mV$_{SCE}$ in 0.1M NaCl, 25°C, R=0.1, a frequency of 1Hz does not enhance the FCG rate over the open circuit potential and air cases, while load frequencies ≤ 0.1Hz do, although the enhancement is not very significant (Figure 3). The effect of environment on the FCG rate can be easily recognized by examining either the correlations between da/dN and f or the correlations between the da/dt and f. If the fatigue crack propagates in a cycle dependent manner, then the FCG rate, da/dN, at each ΔK will have the same value for different load frequencies. Accordingly, the time based log(da/dt) vs. log(f) correlation will be linear, with a slope equal to 1. On the other hand, if an environmental (i.e., time dependent) contribution is important, the value of da/dN for each ΔK will increase with decreasing load frequency, and at low frequencies, the log(da/dt) vs. log(f) curve will deviate upward from a straight line [Figure 4(b)]. The more environmental contribution on the fatigue crack propagation, the more deviation from the linear straight line.

Hicks et al.[8] indicated that internal hydrogen charged Alloy 625 suffered hydrogen embrittlement in room temperature slow strain rate mechanical tests. Tien et al.[9] have developed a model showing that in fatigue of nickel-base alloys at room temperature at a frequency of 1Hz, the dislocation aided hydrogen penetration distance is 7.7 μm. During the hydrogen-assisted cracking, hydrogen would not fundamentally affect the mechanism of crack growth but also enhance it[10]. In this study, the spacing of striations, 1μm measured from Figure 6(c) and the FCG rates are small enough to allow the transport of hydrogen to locations ahead of the growing crack tip. Yet, enhanced crack growth is only observed at f≤0.1Hz. The fractographs show the secondary cracks are found in the 1Hz and 0.1Hz conditions at cathodic charging, and the quantity of the secondary crack in 0.1Hz case is larger than the one in 1Hz case. It is probably that smaller amount of hydrogen existed ahead of the crack tip in 1Hz case just only change the fracture mode but not enhance the crack growth; however, in 0.1Hz case, there are a larger amount of hydrogen not only change the fracture, but also enhance the crack growth.

The enhancement of FCG rates with decreasing frequency during cathodic charging is also found at R=0.2 and 0.5, and the trend is more pronounced as R increases. At high R value, the specimen is under a high mean load and cyclic plastic damage involves a high vacancy concentration which will add to the hydrogen-dislocation interactions and may enhance the hydrogen transport[2]. Besides, the hydrogen produced in the crack will not be pumped out thoroughly during the opening and closing of the crack at high

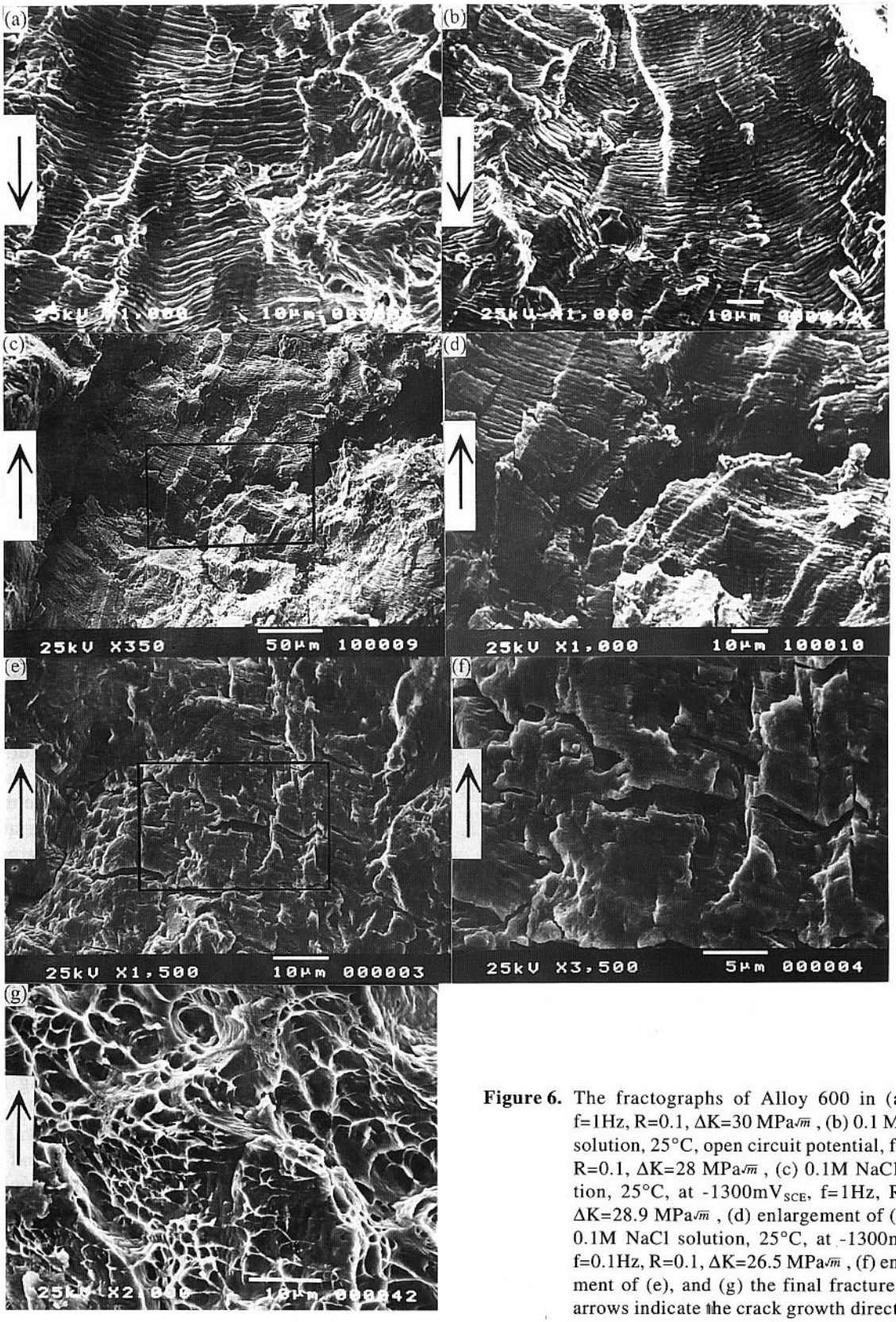

Figure 6. The fractographs of Alloy 600 in (a) air, f=1Hz, R=0.1, ΔK=30 MPa$\sqrt{m}$, (b) 0.1 M NaCl solution, 25°C, open circuit potential, f=1Hz, R=0.1, ΔK=28 MPa$\sqrt{m}$, (c) 0.1M NaCl solution, 25°C, at -1300mV$_{SCE}$, f=1Hz, R=0.1, ΔK=28.9 MPa$\sqrt{m}$, (d) enlargement of (c), (e) 0.1M NaCl solution, 25°C, at -1300mV$_{SCE}$, f=0.1Hz, R=0.1, ΔK=26.5 MPa$\sqrt{m}$, (f) enlargement of (e), and (g) the final fracture. The arrows indicate the crack growth direction.

Table 3. Mechanical properties of mill annealed Alloy 600 in 0.1M NaCl solution, 25°C, at -1300mV$_{SCE}$ with strain rates of 10^{-3} and $10^{-4}s^{-1}$

	0.2% Yield Strength (MPa)	Ultimate Tensile Strength (MPa)	Elong. (%)	Pct. RA (%)
$10^{-3}s^{-1}$	220.0	621.7	65.4	50.0
$10^{-4}s^{-1}$	205.5	622.3	61.4	48.8

R value, therefore there is much more hydrogen retained in the crack. In the case of R=0.5, the test period is longer than the cases of R=0.1 and 0.2; therefore the enhancement exists in the f=1Hz condition, though the frequency is higher than 0.1Hz.

The phenomenon of hydrogen embrittlement is characterized by a loss of the mechanical properties of the materials. In this study, the results of the tension test in 0.1M NaCl solution, 25°C, at -1300mV$_{SCE}$ do not reveal the phenomenon. The crosshead speed, 2.5×10^{-2} mm/sec, is slower than the roughly estimated speed, 2×10^{-1} mm/sec, of the load rising process during the initial stage of the fatigue testing at 0.1Hz. The dislocations are produced homogeneously on the reduced section of the standard specimen under uniaxial load and the plastic zones also distribute homogeneously. Therefore, hydrogen is also distributed homogeneously on the surface of the specimen, and the contribution of hydrogen on the mechanical properties is neglected in comparison with the pure mechanical effect. For the CT specimen, the dislocations and plastic zones are localized in the crack tip region, hydrogen can easily penetrate to the crack. However, the effects of hydrogen are only found in fatigue testing, but not in tension test. Since more dislocations were produced during fatigue testing than uniaxial tensile testing, therefore more hydrogen could be transported to the crack tip during fatigue testing.

The FCG rates of Alloy 600 increased with the load ratio increasing in air and 0.1M NaCl solution at -1300mV$_{SCE}$ (Figure 5). A higher load ratio results in a higher mean load $[(P_{max}+P_{min})/2]$; in addition, this condition would simultaneously cause the FCG rate to increase. It is important to account for the load ratio factor in using the data presented here for structural evaluation, because a typical reactor component will experience a wide range of loading as well as load ratios during its design life. A number of relationships have been proposed to account for the effect of load ratio, two of the more generally employed being those by Forman[11] and Walker[12]. The relationship used here is that by Walker, which involves a portrayal of FCG rate data in terms of an "effective" stress intensity factor, K_{eff}, which is defined as

$$K_{eff}=K_{max}(1-R)^X \quad (3)$$

where

K_{max}=maximum applied stress intensity factor

R=load ratio ($=P_{min}/P_{max}=K_{min}/K_{max}$)

X=an empirical constant dependent on material and environment

The fatigue crack growth law then becomes

$$da/dN=C\times K_{eff}^{n} \quad (4)$$

where C and n are determined from test data. The Walker's model has the added advantage of reducing to the classic ΔK relationship when X=1.0. The results of application of the Walker model with the parameter X=0.2 to the results of this study in 0.1 M. NaCl solution, 25°C, at -1300mV$_{SCE}$ is shown in Figure 7. Note that all the data now almost fall along a single straight line in the logarithmic presentation. The conservative upper bound FCG rate curve, f=0.1Hz, for Alloy 600 in 0.1M NaCl solution, 25°C, at -1300mV$_{SCE}$ is

$$da/dN=1.46\times10^{-16}[K_{max}(1-R)^{0.2}]^{6.91} \quad (5)$$

where

da/dN is in m/cycle

K_{max} is in MPa$\sqrt{m}$

The quantitative models of environmental induced fatigue crack propagation show the interaction of mechanical and environmental fatigue in-

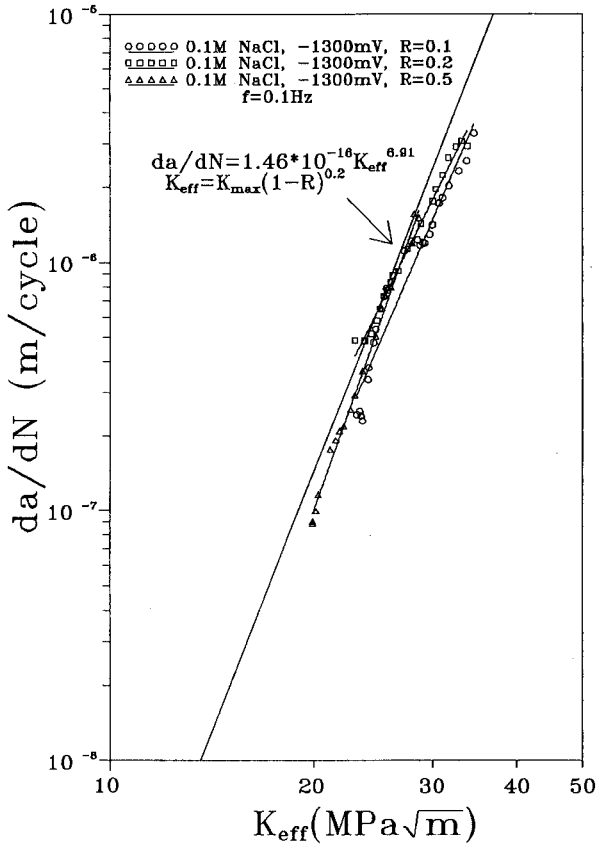

Figure 7. Application of Walker model to correlate the FCG rates, f=0.1Hz, vs. effective stress intensity factor to Alloy 600 in 0.1M NaCl solution, 25°C, at -1300m V_{SCE}, $K_{eff}=K_{max}(1-R)^{0.2}$.

cluding superposition[13] and competition models[14]. The superposition model considers the rate of fatigue crack propagation in an environment which is produced by concurrent parallel processes. For two processes, the superposition concept is then given by the following

$$(da/dN)_e=(da/dN)_m(\theta)+(da/dN)_{cf}(\Phi) \qquad (6)$$

where $(da/dN)_e$ is the total measured crack growth rate in an aggressive environment; $(da/dN)_m$ is the rate of plasticity-driven fatigue crack propagation for an inert environment; $(da/dN)_{cf}$ is the rate due to environmental contribution; θ is the fraction of the crack surface formed by mechanical fatigue; and Φ is the fraction of the crack surface formed by environmental fatigue. The competition model[14], a special case of eq.(6), depicts the above two parts compete with each other during the fatigue process, which one contributes the most to the FCG rate would control the FCG rate under aggressive environment. The test results of this study from the da/dN-ΔK plots show the environmental contribution on the FCG rates of Alloy 600 in NaCl solution at cathodic potential is probably due to the hydrogen embrittlement. From the superposition model's point of view, the fraction (Φ) of the crack surface formed by environmental (hydrogen embrittlement) induced crack is larger than the one (θ) formed by pure mechanical fatigue in the FCG behavior of Alloy 600 in 0.1M NaCl solution, 25°C, at cathodic potential. The value of Φ increases with decreasing the load frequency and also increases significantly with the load ratio being raised. In other words, the hydrogen embrittlement controls the FCG behavior of Alloy 600 in NaCl solution at cathodic potential, from the competition model's point of view.

CONCLUSIONS

The following conclusions could be made on the basis of above discussions:

1. The FCG rates of Alloy 600 increased with decreasing load frequency in 0.1M NaCl solution, 25°C, at -1300mV_{SCE}.
2. The FCG rates of Alloy 600 in air and 0.1M NaCl solution, 25°C, at -1300mV_{SCE} were found to increase with increasing load ratio at any given values of stress intensity factor range, ΔK, and the phenomenon of the enhanced FCG rate at f=0.1Hz was more pronounced with increasing the load ratio.
3. The fractographs at cathodic potential showed brittle fracture mode and the enhancement on the FCG rates of Alloy 600 in 0.1M NaCl solution, 25°C, at -1300mV_{SCE} was probable due to the hydrogen embrittlement.
4. A conservative upper bound FCG rate curve, f=0.1Hz, for Alloy 600 in 0.1 M NaCl solution, 25°C, at -1300mV_{SCE} is

$$da/dN=1.46\times10^{-16}[K_{max}(1-R)^{0.2}]^{6.91}$$

where

da/dN is in m/cycle,

K_{max} is in MPa$\sqrt{m}$.

ACKNOWLEDGMENTS

The authors would like to express their deep appreciation for the financial support of the National Science Council of the Republic of China under contract No. NSC 82-0413-E-007-247, and to thank Prof. J.H. Huang, Department of Nuclear Engineering and Engineerimg Physics, National Tsing Hua University for the discussion in this study.

REFERENCES

1. J.T. Adrian Roberts, Structural Materials in Nuclear Power Systems(Plenum Press, New York 1981) p. 344.
2. G.S. Was, H.H. Tischner, R.M.Latanision, R.M. Pelloux, Metall. Trans. A, 12A (1981)1409.
3. H.M. Shalaby, P. Zhao, G. Cragnolino, D.D. Macdonald, Corro., 44 (1988) 905.
4. R. Bandy, D. Van Rooyen, Corro., 40 (1984) 425.
5. N. Totsuka, E. Lunarska, G. Cragnolino, Z. Szklarska-Smialowska, Corro., 43 (1987) 505.
6. ASTM Standard E-647-83, American Society for Testing and materials, Philadelphia, Pa. (1983).
7. J.T. Ho, G.P. Yu, "Fatigue Behavior of Alloy 600 in NaCl Solution at Room Temperature", J. of Nucl. Mat., submitted.
8. P.D. Hicks, C.J. Altstetter, Metall. Trans. A., 21A (1990) 365.
9. J.K. Tien, R.J. Richards, O. Buck, H.L. Marcus, Scr. Metall., 9 (1975) 1097.
10. C.D. Beachem, Metall. Trans. A, 3A (1972) 437.
11. R.G. Forman, V.E. Kearney, and R.M. Eagle, ASME J. of Basic Engineering, 89, 459 (1967).
12. K. Walker, "The Effect of Stress Ratio During Crack Propagation and Fatigue for 2024-T3 and 7075-T6 Aluminum," Effects of Environment and Complex Load History on Fatigue Life, ASTM STP 462, American Society for Testing Materials (1970) p.1.
13. R.P. Wei, M. Gao, Scripta Metall., 17 (1983) 959.
14. I.M. Austen, and E.F. Walker, in "Mechanisms of Environment Sensitive Cracking of Materials", edited by P.R. Swann et al, London, The Metals Society, (1977) p. 334.